# Tractable Terrain-aware Motion Planning on Granular Media: An Impulsive Jumping Study

Christian M. Hubicki[1], Jeff J. Aguilar[2], Daniel I. Goldman[2] and Aaron D. Ames[3]

*Abstract*— This work demonstrates fast motion planning for robot locomotion that is optimized for terrain with complex dynamics, specifically, rapid penetration of granular media. Gait planning is critical for many legged locomotion control approaches, but they typically assume rigid ground contact. We aim to extend these planning methods to include terrain dynamics we see in the natural world, like sand and dirt, which can both deform and fluidize. Using an *added-mass* description of collective grain motion, we formulated a model of hydrostatic and hydrodynamic terrain effects that is both principled and representable with closed-form dynamics. As a result, we present a model and fast optimization formulation which solves accurate motion plans on granular media with tractable solving times (6.4±3.8 seconds). For validation, we optimized open-loop motor trajectories for a testbed jumping robot to jump to a target apex height from a bed a loosely packed poppy seeds, a model granular medium. While jumps optimized for rigid ground were anemic on granular media, terrain-aware trajectories hit within 6% of their target. This demonstrates the potential for robot locomotion which meets practical task demands, all while being aware of the terrain beneath it.

## I. INTRODUCTION

In pursuit of dynamic walking and running robots, significant progress has been made toward control and motion planning with the nonlinear, hybrid dynamics of legged machines [1], [2], [3]. However, it is less common to study a robot's interactions with the dynamics of the terrain beneath its feet [4], [5]. The world is full of dirt, sand, mud, and other deformable terrain, but by and large, underlying physical models employed in motion planning typically assume rigid contact. Here, we present a tractable method for motion planning subject to rapid interactions with a complex substrate, specifically in loose-packed poppy seeds (a granular medium which has proven useful in the study of complex-terrain locomotion [6], [7]). We experimentally validate our planning on a testbed spring-legged jumping robot (Fig. 1).

Optimal motion planning techniques, such as direct collocation [8], have the power to quickly and precisely design controlled robotic trajectories to near-arbitrary specifications. In fact, optimal motion planning is often at the crux of
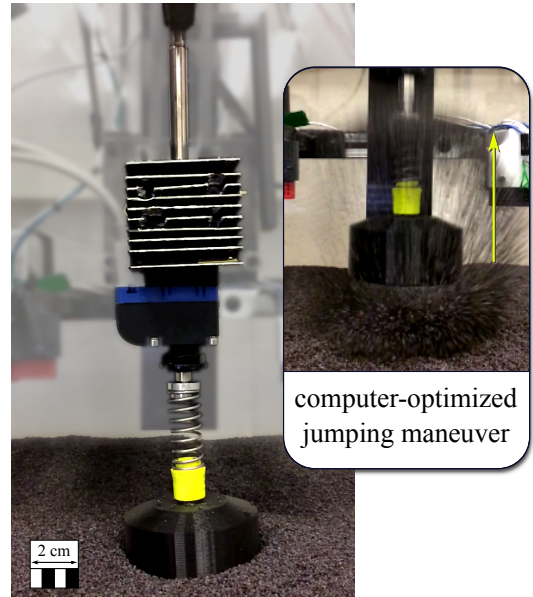


Fig. 1: The testbed robot executing a computer optimized jumping maneuver on loose-packed poppy seeds, an example of granular media (e.g. sand and dirt).

dynamic locomotion control techniques [2], [1]. However, motion planning can be prohibitively slow for practical use if models do not meet certain criteria. Particularly, the model needs to be fast to simulate, or better still, the dynamical equations can be written in closed-form [9], [10]. While the dynamics of robotic links are easy to define in closed-form, granular materials are more challenging to define in a tractable and accurate manner.

Granular media is a complex substrate with both solid- and fluid-like behaviors, and has been described using many methods. While discrete element methods (DEM) can be used to simulate granular media, this reductionist grain-wise modeling approach is time-consuming and computationally expensive, taking several days to compute one second of simulation [6], [11]. Furthermore, such methods do not readily elucidate the underlying principles of granular interaction with robotic locomotors. Simpler spring-damper [12], [13], [14] or viscoplastic [15] dynamics can be employed as a simple proxy model for ground deformations, but these can differ significantly in behavior from granular media. Coulomb friction-based granular force models such as granular resistive force theory (RFT) [6] are computationally efficient tools that provide an empirical description of bulk reaction forces during a variety of complex intrusions. However, such models do not predict reaction forces during high speed

[1]Christian M. Hubicki is with the George W. Woodruff School of Mechanical Engineering, Geogia Institute of Technology, christian.hubicki@me.gatech.edu

[2]Jeff J. Aguilar and Daniel I. Goldman are with the School of Physics, Georgia Institiute of Technology, jeffrey.aguilar@gatech.edu, daniel.goldman@physics.gatech.edu

[3]Aaron D. Ames is with the George W. Woodruff School of Mechanical Engineering and the School of Electrical and Computer Engineering, Georgia Institiute of Technology, aaron.ames@me.gatech.edu

impulsive intrusions such as those produced during jumping maneuvers. For vertical penetrations, granular reaction forces during high speed, but unforced, impacts (e.g. cratering) have typically been described by the sum of frictional depth dependent static forces and inertial drag forces [16], [17], [18].

However, a recent study of jumping on granular media [19] revealed that such force models are insufficient to predict the dynamics of fast modes of locomotion, where intrusions are not only impulsive, but externally forced, leading to more complex interactions with the substrate. The study revealed an added-mass effect, whereby a volume of grains compacts and accumulates below the intruding foot. Hydrostatic and hydrodynamic (both inertial drag and added mass) forces emerge whose properties are determined by the accumulation dynamics and geometry of the compacted volume of grains. Specifically, the jammed grains progress with the geometry of a developing cone. This principled reduced-order formulation can also be represented with closed-form equations, making it amenable to fast motion planning techniques. As such, we employ these added mass dynamics in our terrain model.

To set an aggressive benchmark to test the effective accuracy of our motion plans, we explored the problem of open-loop impulsive jumping on loose-packed grains. Open-loop impulsive jumping presents a number of challenges. By sending only open-loop motor-position commands to the jumper, there is no opportunity to correct errors online. Also, we measure jump accuracy by apex height error, which is sensitive to the error in takeoff velocity[1]. By demanding high jumps which require quick impulsive motions, the granular media will operate in a complex fluidizing domain outside simpler resistive force theory models.

In total, this work presents three experimental groups of impulsive robotic jumping. We test **1)** a trajectory optimized with a rigid ground model, executed on rigid ground, **2)** a trajectory optimized with the added-mass model and executed on loosely packed poppy seeds, and **3)** a trajectory optimized with a rigid ground model, but executed on loosely packed poppy seeds. After comparing target vs. actual hop heights, we will show that optimizing with the added mass model allows the jumper to accurately hit its target apex height within 6.6% error. Further, not only do rigid-ground-optimized strategies come nowhere close to target heights (40.6% error), some strategies optimized for higher jumps underperformed strategies optimized for lower jumps when tested on granular media. This will underscore the fact that successful control on granular media is not just a matter of amplifying rigid-ground strategies, but thoughtfully considering the complex dynamics of the terrain.

## II. MODELING

To test fast and dynamic interactions, we use a spring-legged testbed jumping robot as pictured in Fig. 1 and also

---

[1]Due the ballistic dynamics of the airborne model, errors in hop height scale with the square of the takeoff error.
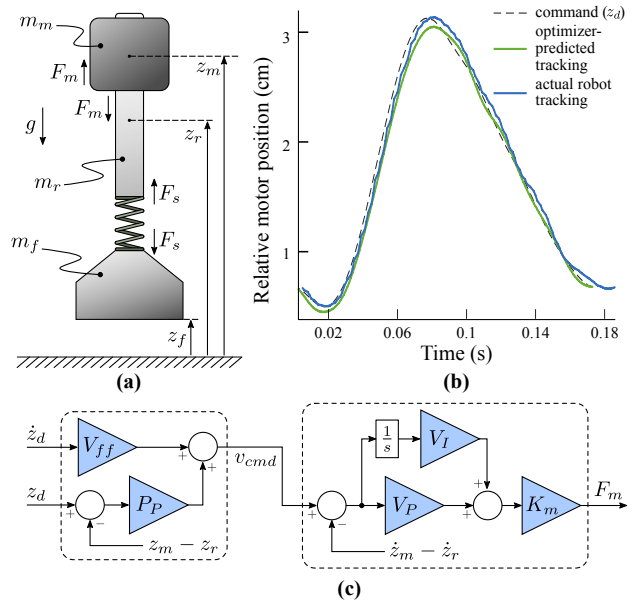


Fig. 2: **(a)** A diagram of the jumping robot math model. **(b)** Motor-to-rod position tracking as predicted by the optimization and measured on the robot. While the tracking error may not appear large, it has a significant impact on the resulting jumping dynamics. **(c)** The motor control feedback loop used to track the open-loop desired actuator position trajectory, $z_d$, such that $z_m - z_r \to z_d$.

described in [19]. The jumper consists of a motor block, rod, and foot, and is constrained to 1D vertical motion via a linear rail. A visualization of the robot math model is shown in Fig. 2a.

### A. Jumping Robot Model

To model jumping, we define the system as a hybrid system with two continuous domains [10]: *stance* ($\mathcal{D}_{st}$) and *flight* ($\mathcal{D}_{fl}$), defining when the robot has its foot on the ground and in the air, respectively (illustrated in Fig. 4a). During stance on rigid ground, we define the equations of motion:

$$\ddot{z}_m = F_m/m_m - g, \tag{1}$$
$$\ddot{z}_r = -F_m/m_r + F_s/m_r - g, \tag{2}$$
$$\ddot{z}_f = 0, \tag{3}$$

where $z_m$, $z_r$, and $z_f \in \mathbb{R}$ denote the vertical position of the motor, rod, and position, respectively, with masses $m_m$, $m_r$, and $m_f$, also respectively. $F_m$ is the linear actuator force and $g$ represents gravitational acceleration ($9.81 m/s$). $F_s$ is the spring force defined as a linear spring with viscous dissipative losses:

$$F_s = k_s(z_f - z_r + l_0) - c_s(\dot{z}_r - \dot{z}_f) \tag{4}$$

where $k_s$ and $c_s$ are the linear stiffness and damping coefficient of the spring, and $l_0$ is the zero force length.

Additionally, we found that the motor-position feedback control loop, as a result of imperfect tracking plotted in

Fig. 2b, had a significant effect on the system dynamics. We write the feedback control equations as:

$$v_{err} = P_P(z_d(t) - (z_m - z_r)) + \qquad (5)$$
$$V_{ff}\dot{z}_d(t) - (\dot{z}_m - \dot{z}_r),$$

$$F_m = K_m(V_P v_{err} + V_I \int v_{err} dt), \qquad (6)$$

where $z_d(t)$ is the open-loop commanded desired motor trajectory, $v_{err}$ is the velocity error, $P_P$, $V_{ff}$, $V_P$, and $V_I$ are controller gains, and $K_m$ is the actuator force constant (3.81 N/A). These feedback dynamics are diagrammed in Fig. 2c. To be clear, even though there is a feedback controller described in the dynamics, the *control is effectively open-loop*. The desired trajectory, $z_d(t)$, is not altered online and there is no online feedback on the overall position of the robot. Essentially, the robot was not given the capability to sense and correct its jumping trajectory if it deviates from the motion plan.

To remain grounded during the stance phase, the ground-reaction force must always be non-negative, $F_s + m_f g \geq 0$, and the model transitions to flight when $F_s + m_f g = 0$. Upon entering flight ($\mathcal{D}_{fl}$), the foot dynamics switch to $\ddot{z}_f = -F_s/m_r - g$, where a $z_f \geq 0$ ensures the foot stays above the rigid terrain. The optimizer terminates the flight dynamics at the CoM apex condition, $m_m \dot{z}_m + m_r \dot{z}_r + m_f \dot{z}_f = 0$.

*B. Granular Media Model*

To model interactions with loosely packed granular media, we implement an added-mass model [19]. Fig. 3 illustrates how a cone of compacted grains grows as an intruding object plunges into a granular substrate, with areas defined as

$$A_{flat}(z_f) = \qquad (7)$$
$$\pi \left( R^2 + \left( \mu \frac{z_f^0 - z_f}{\tan\theta} \right)^2 - 2R\mu \frac{z_f^0 - z_f}{\tan\theta} \right),$$

$$A_{cone}(z_f) = \frac{\pi R^2 - A_{flat}(z_f)}{\cos\theta}, \qquad (8)$$

where $\mu$ is the recruitment rate ($\mu = 2$), and $R$ is the foot radius, and $\theta$ is the shear band angle (60°). As the cone forms, more mass is effectively added to the foot (hence "added mass"). Given these geometric definitions, we can compute the added mass, $m_g$, as

$$m_g = -c_g\phi\rho\mu \int A_{flat}(z_f)dz_f, \qquad (9)$$

where $\phi$ is the volume fraction (0.57, indicating very loose packing), $\rho$ is the grain density (1000 kg/m³ for poppy seeds), and $c_g$ is a surrounding mass scaling factor ($c_g = 2.7$). When we differentiate added mass with respect to time, we get the differential equation:

$$\dot{m}_g = -c_g\phi\rho\mu A_{flat}\dot{z}_f. \qquad (10)$$

This accumulation of mass 1) reduces the acceleration of the foot ($m_g\ddot{z}_f$) and also 2) introduces an inertial term due to the rate of change of the added mass ($\dot{m}_g\dot{z}_f$). Further, we
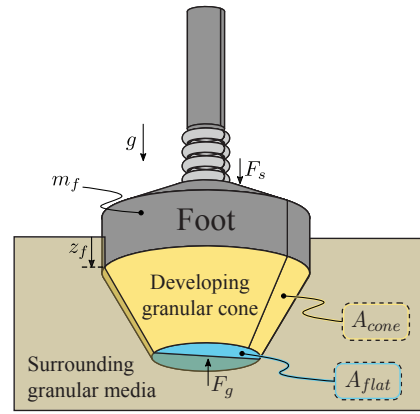


Fig. 3: A visual depiction of the geometry of the added mass as a compacted granular cone develops.

extend the notion of this granular cone to describe hydrostatic forces, which act on the exposed area of the cone ($A_{flat}$ and $A_{cone}$) in a manner which increases with depth. All together, these forces yield a collective granular media force, $F_g$:

$$F_g = \frac{k_{sh}}{\pi R^2} \int A_{flat}(z_f)dz_f + \sigma_{rft} \int A_{cone}(z_f)dz_f \qquad (11)$$
$$- b\dot{m}_g\dot{z}_f - m_g\ddot{z}_f,$$

where $k_{sh}$ is the penetration stiffness (1600 $N/m$), $b$ is the inertial drag scaling factor ($b = 17.2$), and $\sigma_{rft}$ is the depth dependent resistive stress ($0.12 \times 10^6$ N/m³) [6]. The only granular media parameter that was tuned empirically in these experiments was the inertial drag scaling factor, $b$. It was tuned to fit a particular jump height, but kept constant for all other points. All remaining parameters were taken from theory, previous studies [19], or direct measurement.

We can now use this granular media force, $F_m$ in our hopper dynamics, forming our new granular media domain, $\mathcal{D}_g$. During granular stance ($\mathcal{D}_g$), $\ddot{z}_f = F_g/m_r - F_s/m_r - g$, given the constraint that the terrain has no restorative motion, $\dot{z}_f \leq 0$. To transition to flight ($\mathcal{D}_{fl}$), the foot must have zero velocity, $\dot{z}_f = 0$, and must have non-negative acceleration at takeoff, $-F_s - m_f g \geq 0$. A graph illustrating the transitions between stance and flight domains is pictured in Fig. 4b.

## III. OPTIMIZATION

Here, we present an optimization formulation for fast optimal motion planning. By formulating an optimal control problem as a constrained nonlinear program (NLP) [20], we can leverage a well-developed array of NLP solvers (e.g. IPOPT [21]). Further, we use direct collocation methods [8], which facilitate reliable gait optimization [22], [9], [10].

Direct collocation methods work by discarding the simulator which would ordinarily integrate the dynamics, and delegating the role of dynamical integration to the optimizer itself. The optimizer integrates the dynamics by solving a series of algebraic equality constraints at a series of collocation points. More recent work showed the potential for drastic reductions in computation time when the dynamical equations can be written in closed-form. In such cases, all of
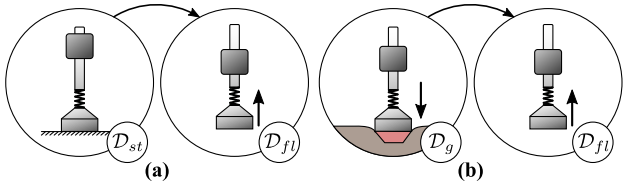
Fig. 4: Flow of continuous domains for **(a)** hard ground jumping and **(b)** jumping on granular media. This domain sequence is explicitly scheduled in the optimization.

the optimization constraints, as well as their Jacobians can also be written in closed-form [9]. This prevents the optimizer from using finite differencing methods to approximate Jacobians, which are computationally taxing. This approach has been streamlined further to optimize 3D walking for a humanoid robot [10].

We build our formulation by discretizing the trajectory in time for each domain (stance and flight):

$$0 = t_0 < t_1 < t_2 < \cdots < t_N = T_I, \qquad (12)$$

where $N$ is the number of nodes defining the trajectory ($N$=31 for all reported cases), and $T_I$ is the final time of the domain. Next, we parse all of our differential equations into a system of first-order differential equations, with state vector, $x$. We discretize all these state variables, $x^i$, for $i \in \{1, 2, 3, \ldots, N-1\}$ and for all domains. For any arbitrary state variable with first order dynamics, $x^i$, we introduce an implicit trapezoidal integration scheme to connect it algebraically to its derivative, $\dot{x}^i$. This is called a *defect constraint*:

$$(x^{i+1} - x^i) - \frac{1}{2}\Delta t^i(\dot{x}^{i+1} + \dot{x}^i) = 0, \qquad (C1)$$

$$\dot{x}^i - f(x^i) = 0, \qquad (C2)$$

where $\Delta t^i = t_{i+1} - t_i$. Here, we use an even nodal spacing, $\Delta t^i = \frac{T_I}{N-1}$. If we can define the first-order system dynamics, $\dot{x} = f(t, x)$, where $f(t, x)$ can be expressed in closed-form, then every defect constraint can also be expressed in closed-form [9]. Now, we build a vector of all optimization variables[2], $\mathbf{y}$,

$$\mathbf{y} = \{z_m^i, \dot{z}_m^i, z_r^i, \dot{z}_r^i, z_f^i, \dot{z}_f^i, \ddot{z}_f^i, \ldots \qquad (13)$$
$$z_d^i, \dot{z}_d^i, \ddot{z}_d^i, e_{int}^i, F_m^i, m_g^i\},$$

and formulate the nonlinear program,

$$\mathbf{y}^* = \underset{\mathbf{y}}{\arg\min} \ \frac{\Delta t}{2} \sum_{i=1}^{N}(\dot{z}_m^i - \dot{z}_r^i)^2 \qquad (14)$$

$$\text{s.t} \qquad \mathbf{y}_{\min} \leq \mathbf{y} \leq \mathbf{y}_{\max}, \qquad (15)$$

$$\mathbf{c}_{\min} \leq \mathbf{c}(\mathbf{y}) \leq \mathbf{c}_{\max}, \qquad (16)$$

where $\mathbf{c}(\mathbf{y})$ represent all constraint functions, including task constraints[3], especially the hop height condition which is the difference in $z_r$ between the start of the jump and apex. The

---

[2]$e_{int}^i$ encodes the numerical integral term, $\int v_{err}dt$, from (6).
[3]Task constraints: $-46N \leq F_m \leq 46N$; $-27.5mm \leq z_m - z_r \leq 27.5mm$; $32.5mm \leq z_r - z_f$.

objective minimizes the square of the actuator velocity, a simple proxy for motor effort[4]. Now we can take analytical Jacobians to speed up the solution of the problem using the large-scale interior point algorithm, IPOPT [21]. We initialize the solver with arbitrary and infeasible initial guesses (e.g. all zeros with a non-zero time duration), and solving typically takes between 1-10 seconds of computation time.

## IV. EXPERIMENTS

Here we describe our experimental data collection process for our three experimental groups. Specifically, **1)** a trajectory optimized with a rigid ground model, executed on rigid ground, **2)** a trajectory optimized with added-mass model and executed on loosely packed poppy seeds, and **3)** a trajectory optimized with a rigid ground model, but executed on loosely packed poppy seeds.

### A. Experimental Setup

The robotic jumper (developed for a systematic study of hard ground dynamics [23]), consists of a Dunkermotoren STA-1104 linear actuator connected to the carriage of an air bearing (total mass, $m_m = 0.948$ kg), providing constrained vertical motion with low friction. The actuator's thrust rod (mass, $m_r = 0.165$ kg) is connected to a coil spring ($k_s = 2730$ N/m), which is connected to a 7.6 cm diameter disc foot ($m_f = 0.044$ kg). The actuator interfaces with a Copley Accelnet amplifier which sends the motor a command current (proportional to force) based on a position and velocity feedback control scheme. This feedback control scheme has a significant effect on the overall robot dynamics (see Fig. 2b), and had to be explicitly modeled. A high speed Point Gray camera was used for real-time tracking of a white plastic ball attached to the top of the thrust rod.

The robot/air bearing assembly was placed inside a bed of 1-mm poppy seeds (Fig. 1). Originally constructed for a systematic robophysics style study of jumping dynamics and high-speed impulsive interactions with dry granular media [19], the apparatus allowed for automated measurement of jumping performance for varied granular preparations and jumping strategies. Prior to each jumping maneuver, a separate motor lifted and suspended the jumper while a 5 hp blower with variable voltage flow control fluidized the granular bed by sending air flow to the bottom of the bed through a Porex flow diffuser. This process reset the state of media from any previous disturbances and produced a loose-packed state with volume fraction ($\phi \approx 0.57$ in poppy seeds). Additional manual mixing during fluidization insured a consistent loose-packed preparation. For rigid ground experiments, we used the same experimental apparatus, but placed a large sheet of particle board on top of the poppy seeds to produce a rigid surface.

## V. RESULTS & DISCUSSION

Robotic jumps were commanded and tested across a range of specified apex heights on both hard ground and loosely-packed poppy seeds. The actual vs. commanded positions

---

[4]Minimizing $F(m)^2$ typically yields highly oscillatory solutions which are difficult to track with fidelity.
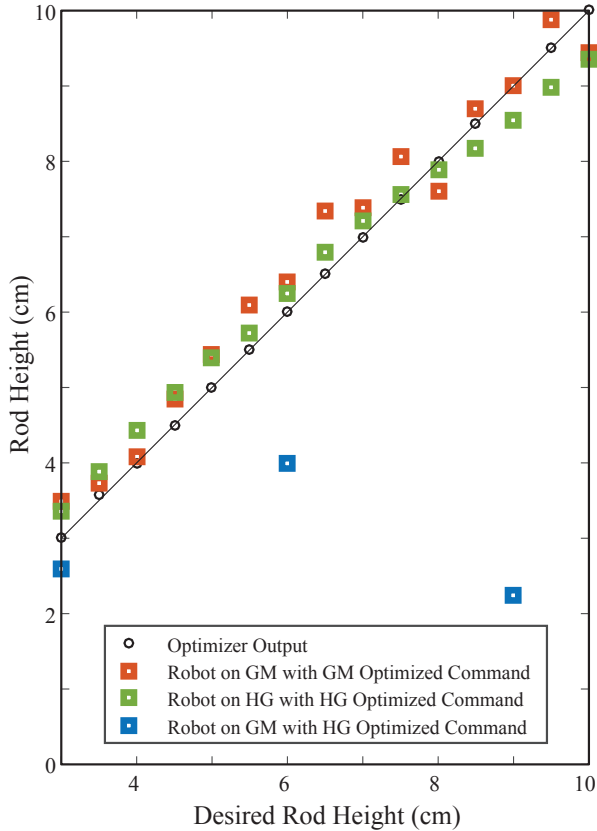
Fig. 5: A plot of actual jumping apex heights vs. commanded apex heights for all three experimental groups. In effect, granular media (GM) command trajectories jumped nearly as accurately on granular media ($3.9 \pm 2.1$ mm) as rigid strategies jumped on hard ground (HG) ($3.4 \pm 1.5$ mm).



Fig. 6: Side-by-side plots of the executed motor trajectories ($z_m - z_r$) optimized for **(a)** rigid ground and **(b)** loosely-packed granular media. Across terrain types, the amplitude and shape of the motor trajectories are clearly distinct. Within terrain types, we observe a smooth shift in strategy with increasing jump height.

of the rod at apex are plotted in Fig. 5. Hard ground strategies jumped to the target apex with an average absolute error of $3.4 \pm 1.5$ mm (mean $\pm$ std dev) when on hard ground (target jump heights range between 30-100 mm). Notably, the granular media trajectories performed similarly (absolute error: $3.9 \pm 2.1$ mm), despite open-loop control and complex terrain dynamics. Executing hard ground strategies on granular media (our experimental control) performed poorly. Not only did the intended 60 mm jump fall short by only reaching 40 mm, attempting a 90 mm jump performed objectively worse and reached just 23 mm. This was the worst performance of all tested jumps.

Inspecting the optimized motor trajectories shows a stark difference in strategies between rigid ground and granular media, plotted in Fig. 6. As commanded jump height increases, the strategy smoothly morphs in shape and amplitude. This suggests that the motion planner is finding meaningful solutions, and not being caught in noisy pseudo-dominima, despite starting from arbitrary and infeasible initial guesses. Unsurprisingly, granular media strategies require more thrust, nearly twice the amplitude compared to counterpart rigid strategies. However, the shape of the motor trajectories is als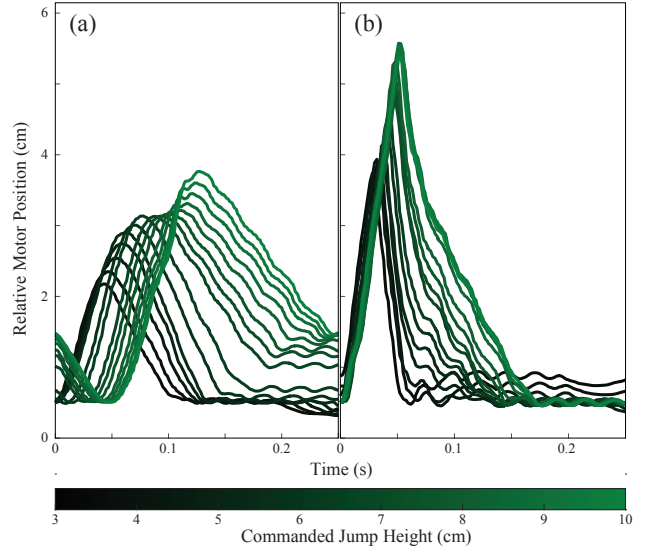o markedly different. Rigid strategies take advantage of a "pull-then-push" strategy, while granular media trajectories favor a single, quick thrust (Fig. 7).

This difference in qualitative strategy likely explains the poor performance of the highest-jumping hard-ground strategies on granular media. Strategies optimized for rigid ground simply do not take the correct shape to leverage granular media dynamics. This emphasizes the importance generating motion plans which are terrain-aware. For instance, if controls engineers heuristically develop a robot controller to jump on sand, they might consider treating the ground as rigid and command a much higher jumping height to compensate for terrain dissipation. These results show that such an approach could perform worse than making no command adjustments at all.

## VI. Conclusions

This study presented and validated a tractable and accurate approach to motion planning through granular media (e.g. sand and dirt) using an added-mass model. Specifically, we tested impulsive jumping on loosely packed poppy seeds to see if we could quickly generate open-loop jumping trajectories which achieve desired apex heights. Our ability to generate optimal jumps on poppy seeds using the added-mass model ($3.9 \pm 2.1$ mm, 6% error) was nearly as accurate in hitting target heights as our jumps on hard ground ($3.4 \pm 1.5$ mm). We believe this is a success of the model and motion planning formulation, especially considering the complex media and open-loop control. Further, using hard ground strategies on granular media was not at all successful. In fact, attempting to jump higher sometimes resulted in even lower jump heights.
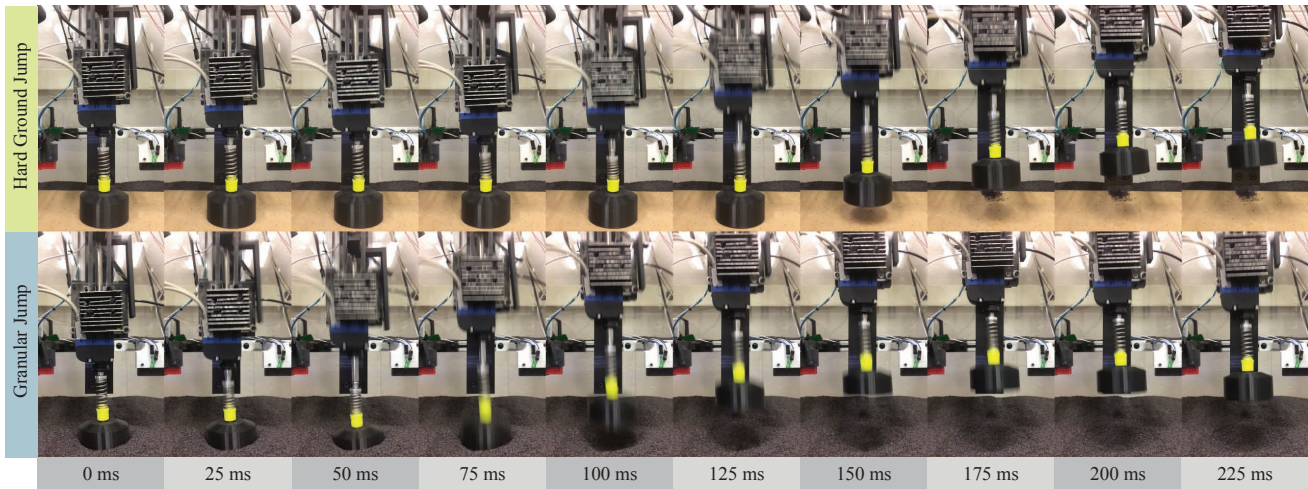
Fig. 7: Tiled images of two 90mm jumps, one on hard ground (top) and the other on loosely packed poppy seeds (bottom).

The computation times are feasible for legged gait design applications and show promise for real-time speeds. Jumping motions were solved in $6.4\pm3.8$ seconds in spite of arbitrary and wildly infeasible initial guesses (a vector of zeros). As reported, these speeds suggest the ability to adapt motion plans to new terrain over the course of a few steps. There are also obvious avenues for improving optimization times (e.g. compiling code in C and improving initial guesses) making sub-second time scales feasible.

Future work will also seek to generalize the terrain model. The presented added-mass model captures the terrain dynamics of a downward thrust with a flat foot, but we suspect other geometries can be accommodated with more-general formulations. In terms of extensibility among substrates (beyond poppy seeds), existing work on terradynamics has shown that the resistive force models for granular media can be linearly scaled across materials [6]. In other words, we expect to model sand and dirt with similar equations.

Overall, these results serve as a proof of concept for the tractability of terrain-aware locomotion control as a general approach. These tools apply to more than 1D jumping, and are a common component of bi- or multi-pedal control. Naturally, the exact control strategies discovered here by the optimizer may not directly apply to an arbitrary legged robot. However, these results demonstrate the sensitivity of optimal legged control to complex substrates, and consequently, the merit of planning with awareness of terrain.

## REFERENCES

[1] E. R. Westervelt, J. W. Grizzle, and D. E. Koditschek. Hybrid Zero Dynamics of Planar Biped Walkers. *IEEE Transactions on Automatic Control*, 48(1):42–56, jan 2003.

[2] I. R. Manchester, U. Mettin, F. Iida, and R. Tedrake. Stable dynamic walking over uneven terrain. *The International Journal of Robotics Research*, 30(3):265–279, 2011.

[3] A. D. Ames. Human-inspired control of bipedal walking robots. *IEEE Transactions on Automatic Control*, 59(5):1115–1130, May 2014.

[4] F. Qian, T. Zhang, W. Korff, P. B. Umbanhowar, R. J. Full, and D. I. Goldman. Principles of appendage design in robots and animals determining terradynamic performance on flowable ground. *Bioinspiration & biomimetics*, 10(5):056014, 2015.

[5] C. Li, S. T. Hsieh, and D. I. Goldman. Multi-functional foot use during running in the zebra-tailed lizard (callisaurus draconoides). *Journal of Experimental Biology*, 215(18):3293–3308, 2012.

[6] C. Li, T. Zhang, and D. I. Goldman. A terradynamics of legged locomotion on granular media. *Science*, 339(6126):1408–1412, 2013.

[7] R. D. Maladen, Y. Ding, P. B. Umbanhowar, A. Kamor, and D. I. Goldman. Mechanical models of sandfish locomotion reveal principles of high performance subsurface sand-swimming. *Journal of The Royal Society Interface*, 8(62):1332–1345, 2011.

[8] O. von Stryk and R. Bulirsch. Direct and indirect methods for trajectory optimization. *Annals of Operations Research*, 37:357–373, 1992.

[9] M. Jones. *Optimal Control of an Underactuated Bipedal Robot*. PhD thesis, 2014.

[10] A. Hereid, E. A. Cousineau, C. M. Hubicki, and A. D. Ames. 3d dynamic walking with underactuated humanoid robots: A direct collocation framework for optimizing hybrid zero dynamics. In *IEEE ICRA*, pages 1447–1454, May 2016.

[11] T. Pöschel and T. Schwager. *Computational granular dynamics: models and algorithms*. Springer Science & Business Media, 2005.

[12] C. M. Hubicki and J. W. Hurst. Running on soft ground: simple, energy-optimal disturbance rejection. In *Proc 15th Int Conf on Climbing and Walking Robots (CLAWAR)*, volume (accepted), 2012.

[13] D. Koepl and J. Hurst. Impulse Control for Planar Spring-Mass Running. *Journal of Intelligent & Robotic Systems*, 2:1–15, sep 2013.

[14] H-j Kang, K. Hashimoto, K. Nishikawa, E. Falotico, H-o Lim, A. Takanishi, C. Laschi, P. Dario, and A. Berthoz. Biped walking stabilization on soft ground based on gait analysis. In *2012 4th IEEE RAS & EMBS International Conference on Biomedical Robotics and Biomechatronics (BioRob)*, number 2, pages 669–674. Ieee, jun 2012.

[15] V. Vasilopoulos, I. Paraskevas, and E. G. Papadopoulos. Compliant Terrain Legged Locomotion Using a Viscoplastic Approach. (Iros):4849–4854, 2014.

[16] H. Katsuragi and D. J. Durian. Unified force law for granular impact cratering. *Nature Physics*, 3(6):420–423, 2007.

[17] L. S. Tsimring and D. Volfson. Modeling of impact cratering in granular media. *Powders and grains*, 2:1215–1223, 2005.

[18] P. Umbanhowar and D. I. Goldman. Granular impact and the critical packing state. *Physical Review E*, 82(1):010301, 2010.

[19] J. Aguilar and D. I. Goldman. Robophysical study of jumping dynamics on granular media. *Nature Physics*, 2015.

[20] A.V. Rao. A survey of numerical methods for optimal control. *Advances in the Astronautical Sciences*, 135(1):497–528, 2009.

[21] A Wächter, LT Biegler, YD Lang, and A Raghunathan. Ipopt: An interior point algorithm for large-scale nonlinear optimization, 2002.

[22] W. Xi, Y. Yesilevskiy, and C. D. Remy. Selecting gaits for economical locomotion of legged robots. *The International Journal of Robotics Research*, 2015.

[23] J. Aguilar, A. Lesov, K. Wiesenfeld, and D. I. Goldman. Lift-off dynamics in a simple jumping robot. *Physical review letters*, 109(17):174301, 2012.